Macromolecules

Article

pubs.acs.org/Macromolecules

Robust Biopolymeric Supramolecular "Host–Guest Macromer" Hydrogels Reinforced by *in Situ* Formed Multivalent Nanoclusters for Cartilage Regeneration

Kongchang Wei,[†,‡] Meiling Zhu,[†] Yuxin Sun,[§] Jianbin Xu,[†,‡] Qian Feng,[†] Sien Lin,[§] Tianyi Wu,[§] Jia Xu,[⊥] Feng Tian,[#] Jiang Xia,[¶] Gang Li,[§] and Liming Bian*[,†,‡,%,∥]

[†]Department of Mechanical and Automation Engineering, Division of Biomedical Engineering, [‡]Shun Hing Institute of Advanced Engineering, [§]Department of Orthopaedic and Traumatology, Prince of Wales Hospital, Hong Kong, [¶]Department of Chemistry, and [∥]Shenzhen Research Institute, The Chinese University of Hong Kong, Shatin, Hong Kong

[⊥]Shanghai Jiaotong University Affiliated Sixth People's Hospital, Shanghai, China

[#]Shanghai Institute of of Applied Physics, Chinese Academy of Sciences, Shanghai, China

[%]China Orthopedic Regenerative Medicine Group (CORMed), Shanghai, China

Supporting Information

ABSTRACT: Biopolymer-based supramolecular hydrogels cross-linked by host–guest interactions are usually mechanically weak as shown in "inverted vials" instead of freestanding 3D constructs. Herein, we describe a novel host–guest macromer (HGM) approach for preparation of biopolymer-based freestanding supramolecular hydrogels. Host–guest macromers are formed by molecular self-assembly between adamantane-functionalized hyaluronic acid (AD_xHA) guest polymers and monoacrylated β-cyclodextrins (mono-Ac-βCD) host monomers. Supramolecular hydrogels are readily prepared by UV-induced polymerization of the preassembled host–guest macromers. Such hydrogels are soely cross-linked by *in situ* formed multivalent host–guest nanoclusters and show significantly reinforced mechanical properties yet still retain desirable supramolecular features. They can self-heal and be remolded into freestanding 3D constructs which afford effective protection on the encapsulated stem cells during the compression remolding, making them promising carriers for therapeutic cells that can quickly adapt to and integrate with surrounding tissues of the targeted defects. We demonstrate that such hydrogels not only sustain extended release of encapsulated proteinaceous growth factors (TGF-β1) but also support chondrogenesis of the human mesenchymal stem cells (hMSCs) and promote cartilage regeneration in a rat model.

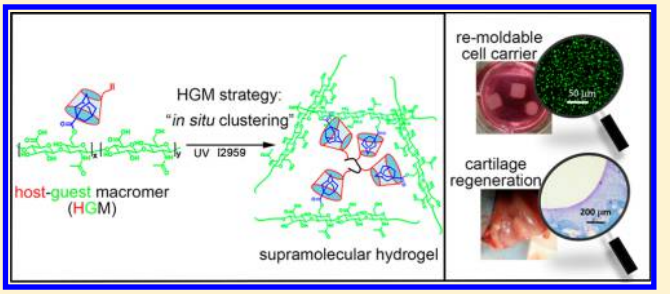

1. INTRODUCTION

Biopolymer-based hydrogels are widely used to emulate the extracellular matrix (ECM) for controlling stem cell differentiation and tissue regeneration because of the similarity between such hydrogels and native ECM in terms of their physical and biochemical properties.[1,2] Although biopolymer-based chemical hydrogels, with biopolymers covalently cross-linked, have been widely used as scaffolds for tissue engineering due to good stability, their permanent network structures and brittleness limit their applications in repairing load-bearing tissues, such as cartilage.[3] In contrast, biopolymer-based supramolecular hydrogels, which are usually formed via self-assembly of physically interacting biopolymers, are usually weak and less stable than chemical hydrogels.[4,5] In spite of their mechanical weakness, biopolymer-based supramolecular hydrogels are attractive biomaterials due to their dynamic network structures. These hydrogels may better emulate the native ECM, within which biopolymers such as hyaluronic acid (HA), collagens, and proteoglycans are mostly interconnected by physical interactions rather than chemical bonding.[6−8] Meanwhile, the reversible nature of their physical cross-links can give rise to useful physical properties, such as self-healing and shear-thinning, which are desirable in biomedical applications of hydrogels.[9−13]

Biopolymers can be cross-linked by many physical interactions, including host–guest complexation, to form supramolecular hydrogels.[14−18] Cyclodextrin-based host–guest interactions are of great interest due to the specificity and effectiveness of host–guest molecular recognition under the physiological condition.[19] However, biopolymer-based host–guest hydrogels are usually feeble and sloppy as shown in the "inverted vials" instead of freestanding 3D constructs,[11] even when bivalent mode host–guest cross-linking was used.[18] Such mechanical weakness significantly limits their widespread

Received: November 23, 2015
Revised: January 10, 2016

ACS Publications © XXXX American Chemical Society

DOI: 10.1021/acs.macromol.5b02527
Macromolecules XXXX, XXX, XXX−XXX

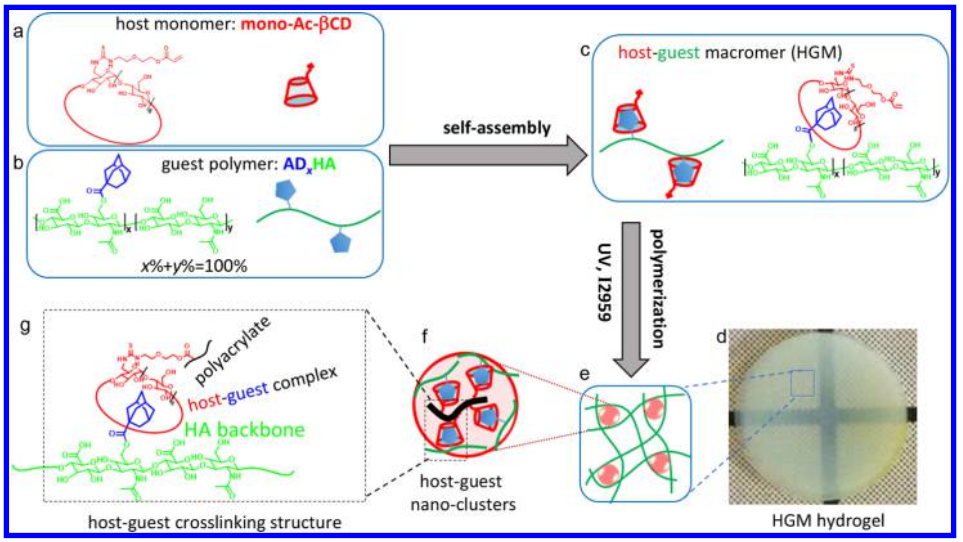

Figure 1. Chemical structures and schematic illustrations of (a) the host monomer (mono-Ac-βCD), (b) the guest polymer (AD$_x$HA), and (c) the host−guest macromer (HGM). (d) The typical translucent appearance of the freestanding HGM hydrogel (4 wt % AD$_{40}$HA). (e) Schematic illustration of the polymer network of HGM hydrogel cross-linked by the host−guest nanoclusters. (f) Schematic illustration of the *in situ* formed host−guest nanoclusters as network cross-linking domains. (g) Chemical structure of the host−guest cross-linking domains.

biomedical applications and could be due to the following two reasons. First, compared to chemical bonding, host−guest interaction is intrinsically weak cross-linking force.[4] Second, the restricted mobility of hosts and guests conjugated to bulky biopolymer backbones will compromise the host−guest complexation properties due to the unfavorable entropy of binding.[18,20] It has been proved that host−guest cross-linkers preassembled from cyclodextrin monomers and adamantane monomers can significantly reinforce the corresponding supramolecular hydrogels, probably due to the more favorable complexation properties of small molecular host/guest monomers comparing to macromolecular host/guest polymers.[21,22] Such preassembled host−guest cross-linkers can be applied to many hydrophilic momoners for preparing host−guest supramolecular hydrogels. However, they are not suitable for physical cross-linking of biopolymer macromers, which are chemically functionalized with multiple polymerizable groups. Such biopolymer macromers can be chemically cross-linked upon polymerization, thus leading to the formation of chemical hydrogels rather than supramolecular hydrogels.To overcome the aforementioned challenges and reinforce biopolymer-based host−guest hydrogels, we develop the host−guest macromer (HGM) approach.

In this study, the selected biopolymer is hyaluronic acid (HA), which is functionalized by adamantane (AD) to form the guest polymer AD$_x$HA (x denotes different modification degrees). β-Cyclodextrin (βCD) is monofunctionalized with polymerizable acrylate (Ac) to form the host monomer, mono-Ac-βCD (Figure 1a,b). First, the photo-cross-linkable host−guest macromers (HGMs) are formed via molecular self-assembly between AD$_x$HA and mono-Ac-βCD driven by the host−guest interaction (Figure 1c). Because the host monomers are less bulky than host polymers, the host−guest complexation is expected to be more efficient than that between host polymers and guest polymers. Subsequently, supramolecular hydrogels (termed HGM hydrogels) are generated by using conventional UV curing. UV-initiated polymerization of the acrylates leads to *in situ* clustering of the preassembled host−guest complexes. The host−guest nanoclusters act as the multivalent cross-linkers of the freestanding HGM hydrogels (Figure 1e−g). Such hydrogels are robust enough to be dried and reswelled to their original shapes repeatedly but still retain the desirable physical properties such as self-healing, compressible, and rapid stress relaxation. By virtue of such supramolecular features, the HGM hydrogels can be remolded to different shapes without compromising the viability of the encapsulated cells, making them ideal cell carrier materials for repairing tissue defects of irregular geometries. We demonstrate that such HGM hydrogels effectively suppress the fast leakage of encapsulated proteinaceous growth factors (TGF-β1) and support chondrogenesis of the human mesenchymal stem cells (hMSCs) and promote cartilage regeneration in a rat model.

2. EXPERIMENTAL SECTION

2.1. Materials. Sodium hyaluronic acid (HA-Na, 74 kDa) was purchased from Lifecore (Chaska, MN). 6-Monodeoxy-6-monoamino-β-cyclodextrin (βCD-NH_2) was purchased from Cyclodextrin-Shop of AraChem. 1-Adamantaneacetic acid, 1-adamantanamine hydrochloride (AD-NH_3Cl), 4-dimethylaminopyridine (DMAP), carbon disulfide, 2-(2-hydroxyethoxy)ethylamine, and acryloyl chloride were purchased from Aladdin. Triethylamine (TEA), methacrylic anhydride (94%), hydrogen peroxide, bovine serum albumin (BSA), and Dowex (50WX8 hydrogen form, 100−200 mesh) were purchased from Sigma-Aldrich. Tetrabutylammonium hydroxide (TBAOH), dimethyl sulfoxide (DMSO), and dichloromethane (DCM) were purchased from Fisher Scientific. Di-*tert*-butyl dicarbonate (BOC_2O) was purchased from TCI. Chloroform-*d* ($CDCl_3$), DMSO-d_6, and deuterium oxide (D_2O) were purchased from J&K. The BCA protein quantification kit was purchased from Life Technologies. Mercapto-β-cyclodextrin was purchased from Shandong Binzhou Zhiyuan Biotechnology Co., Ltd.

2.2. Characterization. All ^{1}H NMR spectra were recorded with a Bruker Advance 400 MHz spectrometer at room temperature. Nuclear Overhauser enhancement spectroscopy (NOESY) experiments were performed using a mixing time of 300 ms, 256 t_1 increments, and 16 scans per t_1 increment on the same spectrometer as that of ^{1}H NMR.

The isothermal titration experiments were carried out on a MicroCal iTC200 isothermal titration calorimeter (ITC) at 25.00 ± 0.01 °C. The high viscosity and the gelation potential of the mixtures of the host polymers and guest polymers preclude the use of polymers at high concentration.[18] Therefore, the binding between the guest

DOI: 10.1021/acs.macromol.5b02527
Macromolecules XXXX, XXX, XXX−XXX

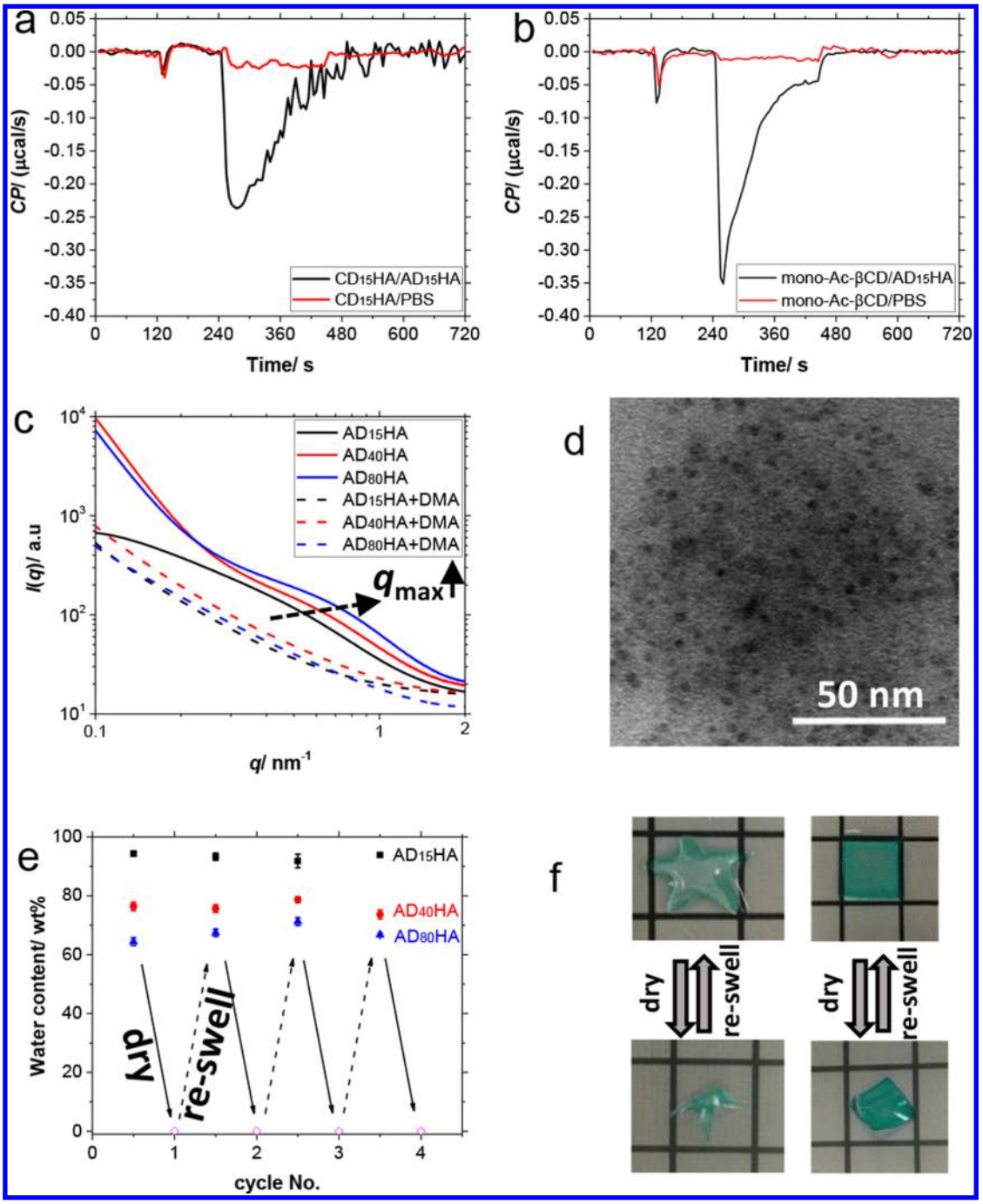

Figure 2. Single injection mode ITC (isothermal titration calorimetry) using (a) the host polymer $CD_{15}HA$ or (b) the host monomer mono-Ac-βCD to titrate guest polymer $AD_{15}HA$ (control titrations are also shown with PBS titrated by host monomer or host polymer, red curves). (c) SAXS profiles of the equilibrium-swollen HGM hydrogels with or without *N*,*N*-dimethylacrylamide (DMA) as comonomer. (d) TEM image of the multivalent cross-linking domains of host−guest nanoclusters in HGM hydrogel matrix. (e) The maintenance of the water content in the HGM hydrogels after cyclic drying−swelling procedures. (f) The reproducible shapes of the swollen HGM hydrogels ($AD_{40}HA$) after the drying−swelling cycles (the side length of the square grid is 1 cm).

polymer and host polymer was studied at low polymer concentrations in order to avoid gelation or significant increase in viscosity. Therefore, single injection mode titration was used because a single large injection can generate clearer and more significant signals than multiple small injections of highly dilute titrants. The concentration of the guest polymer $AD_{15}HA$ was fixed at 1.7 μM (containing 0.3 mM of HA disaccharide units) in the ITC sample cell (200 μL). The host monomer, mono-Ac-βCD, or host polymer, $CD_{15}HA$, containing an equal amount of βCD (0.225 mM), were used to titrate $AD_{15}HA$ in one single injection (40 μL), respectively.

Dynamic viscoelasticity of the hydrogels was measured by an Anton Paar MCR301 rheometer equipped with a 25 mm plate−plate. For oscillatory time sweep experiments, the constant strain and frequency were fixed at 1% and 10 Hz, respectively. For oscillatory frequency sweep experiments, the constant strain was fixed at 1%. For oscillatory strain sweep experiments, the constant frequency was fixed at 10 Hz. For 3ITT (3-interval time test) experiment, the strain was controlled at 10%, 300%, and 10% for the three intervals while the frequency was fixed at 10 Hz.

DOI: 10.1021/acs.macromol.5b02527
Macromolecules XXXX, XXX, XXX−XXX

Compression tests of the hydrogels were conducted on a MACH-1 micromechanical system. Disk-shaped hydrogel samples (d = 5 mm, h = 2 mm) were made in custom-made molds and compressed at a fixed rate of 0.04 mm/s to the target strain levels.

Synchrotron radiation small-angle X-ray scattering (SAXS) experiments were performed on the BL16B beamline of the Shanghai Synchrotron Radiation Facility (SSRF). The sample-to-detector distance was 2000 mm, and the X-ray wavelength was λ = 0.124 nm. 2D SAXS data were converted into 1D intensity $I(q)$ as a function of scattering vector q [$q = (4\pi/\lambda) \sin\theta$] by circular averaging, where 2θ is the scattering angle. A hydrogel specimen with a disk shape (d = 5 mm, h = 1 mm) was used for SAXS analysis.

The TEM images were acquired by using a Hitachi H7700 transmission electron microscope. Samples were prepared by directly pressing carbon-coated TEM support grids onto the hydrogels to remove a thin film of hydrogel matrix for further observation.[44]

2.3. Synthesis of Guest Polymers AD$_x$HA. AD$_x$HA (x% represents the degree of functionalization, i.e., the percentage of the modified disaccharide repeating units of HA) was synthesized according to the reported method with minor modification.[11] As illustrated in Figure S1, first, sodium hyaluronic acid (HA-Na, 2.0 g) was treated by Dowex resin (6.0 g) for ion exchange in the water phase and then neutralized by tetrabutylammonium hydroxide (TBAOH) to produce the HA-TBA aqueous solution (pH = 7), which is soluble in DMSO after lyophilization. Second, HA-TBA (1.0 g, 1.4 mmol disaccharide repeat units, 1 equiv), 1-adamantaneacetic acid (0.82 g, 4.2 mmol, 3 equiv), and 4-dimethylaminopyridine (DMAP, 0.13 g, 1.05 mmol, 0.75 equiv) were dissolved in 100 mL of anhydrous DMSO at room temperature, and di-*tert*-butyl dicarbonate (BOC_2O, y equiv) was added slowly under nitrogen protection at room temperature. The mixture was heated to 45 °C and kept for 24 h. After cooling down to room temperature, the reaction mixture was directly dialyzed against DMSO, NaCl(aq), and then DI water to remove all unreacted small organic compounds. The solution was then frozen and lyophilized to yield the product as a white solid. The degree of modification (x% = 15%, 40%, or 80% according to y = 0.4, 0.6, or 0.8) was quantified by ^{1}H NMR (Figures S2−S4) from the integration ratio between the ethyl multiplet of adamantane (δ = 1.50−1.85, 12H) and the HA backbone (δ = 3.20−4.20, 10H).

2.4. Synthesis of the Host Monomer, Mono-Ac-βCD. Mono-Ac-βCD was synthesized according to Figure S5. Briefly, the amino group of 2-(2-hydroxyethoxy)ethylamine was first converted to isothiocyanate according to the previously reported method,[43] yielding the intermediate *HO-NCS* (confirmed by ^{1}H NMR in Figure S6). The hydroxyl groups of the *HO-NCS* were converted to acrylates by reacting with acryloyl chloride, thereby yielding *Ac-NCS* (confirmed by ^{1}H NMR in Figure S7). To synthesize mono-Ac-βCD, equivalent *Ac-NCS* was mixed with βCD-*NH*$_2$ in DMSO. The crude product was precipitated in acetone after 12 h and purified by repeating the precipitation in acetone three times. The coupling efficiency was characterized by ^{1}H NMR (Figure S8, around 85%), and the molecular weight (M_w 1334 Da) was confirmed by MALDI-TOF MS ($M^+ + Na^+$: 1357, Figure S9).

3. RESULTS AND DISCUSSION

3.1. Fabrication of the Host−Guest Macromer Hydrogels. UV-mediated photo-cross-linking has been commonly used to prepare chemical hydrogels from biopolymers due to its excellent temporal and spatial control.[23−25] Biopolymers used for photo-cross-linking are usually chemically functionalized with polymerizable groups, such as acrylates, acrylamides, methacrylates, methylacrylamides, etc., on their backbones, yielding the photo-cross-linkable macromers.[26−28] Photo-cross-linking of such macromers produces biopolymer hydrogels cross-linked by hydrophobic domains of synthetic polymer backbones such as polyacrylates corresponding to the grafted polymerizable functional groups.[29−31]

Herein we use the photo-cross-linkable host−guest macromers (HGMs) instead of conventional chemical macromers (Figure 1). We choose HA as the biopolymer backbone because it is a key structural component in native extracellular matrix (ECM) and an influential regulating factor of cellular behaviors.[27,32] β-Cyclodextrin (βCD) is used as the supramolecular host to complex with the guest adamantane (AD) for its well-known biocompatibility, good water solubility, and appreciable binding strength.[33,34] AD-functionalized guest polymer AD$_x$HA is synthesized by simple esterification reaction.[11] x denotes the modification degree of AD. Guest polymers with low (x = 15), medium (x = 40), and high (x = 80) modification degree are prepared (Figures S1−S4). In order to avoid chemical cross-linking generated from the photoinitiated radical reaction during gelation, we have designed and synthesized the host monomer with exactly one acrylate group. The amine reactive isothiocyanate derivative (*HO-NCS*) is first acrylated by acryloyl chloride to yield *Ac-NCS*, which is then coupled to the only amine group of 6-monodeoxy-6-monoamino-β-cyclodextrin (βCD-*NH*$_2$), yielding the mono-Ac-βCD host monomer (Figures S5−S9). By simply dissolving AD$_x$HA and mono-Ac-βCD in the same PBS (pH 7.4) solution, the HGMs are formed driven by the specific host−guest complexation as verified by the NMR analysis (Figures S13 and S14). Upon complexation, the chemical shift of the ethyl multiplet of AD changes significantly, and the corresponding peak is broadened. The specific host−guest interaction is further confirmed by 2D NOESY NMR, where the AD proton peaks are found correlated with the inner protons (C(3)-*H* and C(5)-*H*) of βCD.

During the conventional preparation of host−guest hydrogels, the direct self-assembly of host polymers and guest polymers entails the decrease of host−guest complexation properties due to the unfavorable entropy of binding.[17] In contrast, our HGM approach produces more efficient and thorough host−guest complexation between the freely diffusing host monomers and guest polymers as evidenced by the ITC (isothermal titration calorimetry, Figure 2a,b) studies.[35,36] Because of the requirement of ITC testing that no precipitates should be formed during titration, the final concentration of the host polymer CD$_{15}$HA (see Figures S10−S12 for synthesis and characterization) and guest polymer AD$_{15}$HA is fixed at 1.7 μM (0.024 wt % of polymers in the final solution after titration), which is far lower than that used to form the hydrogels. In spite of this, the presence of the HA backbone apparently impairs the host−guest complexation as evidenced by the slow and noisy generation and recovery of the exothermic signal during the titration of guest polymer with host polymers (Figure 2a). In contrast, the quick and smooth generation and recovery of the exothermic signal during the titration of guest polymers with host monomers indicates that the host−guest complexation is more efficient and thorough (Figure 2b). This finding is in agreement with the reported results of the decreased complexation properties of βCD and AD when fixed on the polysaccharide backbone.[17] This efficient host−guest complexation is essential to the formation of the cross-linkable HGMs and the subsequent UV induced hydrogelation. Lastly, freestanding HGM hydrogels are readily created with varied AD$_x$HA concentration (1, 2, and 4 wt %). The low solid content of the HGM hydrogels (only 1.4 wt % for AD$_{15}$HA hydrogels, Figure S15a) demonstrates the efficacy of the HGM strategy in preparing robust supramolecular hydrogels. Such robustness is attributed to the multivalent host−guest cross-

DOI: 10.1021/acs.macromol.5b02527
Macromolecules XXXX, XXX, XXX−XXX

linkers produced by the polymerization of acrylates on the preassembled host–guest complexes. The host–guest nanoclusters, rather than the spatially isolated host–guest complexes obtained from the self-assembly of host polymers and guest polymers, act as the multivalent cross-linkers for HA polymer chains (Figure 1e–g).

3.2. Nanostructure and Robustness of the Host–Guest Macromer Hydrogels. The host–guest clusters form nanometer scale heterogeneity in the HGM hydrogel matrix, and this is similar to the heterogeneous domains in the chemical hydrogels prepared from UV cross-linked macromers.[37] Such heterogeneity is reflected by the translucent appearance of the HGM hydrogels (Figure 1d). We use small-angle X-ray scattering (SAXS) and transmission electron microscopy (TEM) to study the nanostructure of the HGM hydrogels (Figure 2c,d).[37,38] The heterogeneous domains of host–guest nanoclusters are formed during UV-induced polymerization of the HGMs with the host–guest complexes randomly preorganized along the HA chains since the AD functionalization of HA is not position specific. Accordingly, SAXS analysis shows broad correlation peaks within the q (scattering vector, $q = (4\pi/\lambda) \sin \theta$) range from 0.4 to 1 nm^{-1} (Figure 2c). Such broad peaks are attributed to the random distribution of scattering centers in the HGM hydrogel matrix. The peak positions depend on the modification degree of AD_xHA. The peak center shifts to higher q values for higher modification degrees. By using Bragg's law (eq 1)

$$d = \frac{\lambda}{2 \sin \theta} = \frac{2\pi}{q_{max}} \quad (1)$$

where d is the spacing between the scattering centers and q_{max} is the peak positions, we can estimate the spacing between the host–guest nanoclusters (Table 1). In accordance with the shorter HA chain length between adjacent ADs, the nanocluster spacing is smaller for AD_xHA with higher x. By adding a certain amount of *N*,*N*-dimethylacrylamide (DMA, 1 M) as the comonomer during the polymerization of the HGMs, we are able to reduce the clustering effect and to more evenly disperse the copolymerized host–guest complexes in the hydrogel matrix, thereby leading to the disappearance of the correlation peaks (Figure 2c, AD_xHA + DMA). This phenomenon confirms that the heterogeneous scattering centers are host–guest nanoclusters formed by UV-induced radical polymerization.

Table 1. Nanostructural Parameters of the HGM Hydrogels Prepared with AD_xHA[a]

x	n[b]	q_{max} (nm^{-1})	d (nm)	d^* (nm)	d^*/d
15	28	0.56	11.21	6.25	0.57
40	74	0.65	9.66	2.43	0.26
80	148	0.75	8.37	1.23	0.15

[a] x% denotes the modification degree of hyaluronic acid (HA, M_{HA} = 74 kDa). [b] n denotes the average number of AD residues per chain, $n = (M_{HA}/400) \times x\%$.

The TEM examination also indicates the existence of sub-10 nm heterogeneous domains of host–guest nanoclusters in the HGM hydrogel matrix (Figure 2d). Considering that HA polymer backbone is a rigid chain and the length of each disaccharide unit is about 1.04 nm, the averaged chain length between adjacent ADs can be described as $d^* = 100/(x + 1)$ nm.[39] The comparison between d and d^* is summarized in Table 1. The value of d^*/d reflects the conversion ratio of host–guest complexes to host–guest nanoclusters. If the conversion ratio is 100% so that every grafted AD contributes to the host–guest nanoclusters, d^*/d should be close to 1. Incomplete conversion leaves some ADs excluded from the host–guest nanoclusters and gives rise to a larger intercluster spacing than the inter-AD spacing, i.e., $d^*/d < 1$. It is noteworthy that freestanding hydrogels are formed even at low conversion ratios, i.e., low concentrations of multivalent nanoclusters, and a substantial amount of host–guest complexes remains isolated from the nanoclusters. This demonstrates the robustness of the host–guest nanoclusters as the multivalent cross-linkers in reinforcing the supramolecular hydrogels. The reinforcing effect of the host–guest clusters is also demonstrated by the maintenance of the initial water contents and shapes after repeated drying and swelling of the HGM hydrogels (Figure 2e,f). Such robustness enables the convenient storage of the dried hydrogels and the easy use of the reswelled hydrogels and is rarely seen in conventional host–guest polymeric hydrogels.

3.3. Supramolecular Feature of the Host–Guest Macromer Hydrogels. *3.3.1. Physical Nature of the Interpolymer Cross-Linking.* Along with the reinforced mechanical strength, the desirable supramolecular features of the HGM hydrogels are still retained. It is noteworthy that the preformation of HGMs via molecular self-assembly is critical for the HGM hydrogel preparation because the reversed preparation procedure, in which the mixture solution of mono-Ac-βCD and photoinitiator is UV-irradiated prior to mixing with AD_xHA, fails to generate hydrogels (Figure 3a, "reversed-HGM" strategy). Moreover, the addition of competitive guests (i.e., AD-NH_3Cl) into the HGM solution (Figure 3a, competitive inhibition) also effectively blocks the hydrogel formation. These results confirm that the HA polymers are solely cross-linked by the host–guest clusters at the AD-modified positions. Such network structure is also evidenced by the identical swelling kinetics of the HGM hydrogels composed of the AD_xHA with the same AD modification degree (Figure S15b,c). Moreover, dynamic oscillatory rheological studies show that both the storage modulus (G') and damping factor ($\tan \theta = G''/G'$) of the HGM hydrogels are frequency dependent in contrast to the frequency independency of the MeHA hydrogel (prepared from methacrylated HA with 37% modification degree, Figure S11) properties (Figure 3b,c). This finding indicates that HA polymers are physically cross-linked by reversible host–guest interactions in HGM hydrogels. The strain sweep shows that such physically cross-linked HGM hydrogels have a broad linear viscoelastic region without rupture before reaching the strain of 10% (Figure 3d). Such good processability can be attributed to the reversible nature of the host–guest interactions, which enables the dissociated hosts and guests moieties to meet neighboring complementary parts and re-form the host–guest cross-links, thus preventing the polymer network from early rupture.

3.3.2. Compressive Properties of the HGM Hydrogels. More importantly, the reversible nature of the host–guest interactions allows for easy chain rearrangement and reassociation upon compression. Therefore, unlike the brittle chemical MeHA hydrogels, the HGM hydrogels are compressible with much faster stress relaxation rate. MeHA hydrogels are brittle and rupture below 50% strain. In contrast, the HGM hydrogels (4 wt % AD_xHA) are capable of withstanding a much greater strain, up to at least 80% (Figure 4a). In contrast to the

DOI: 10.1021/acs.macromol.5b02527
Macromolecules XXXX, XXX, XXX–XXX

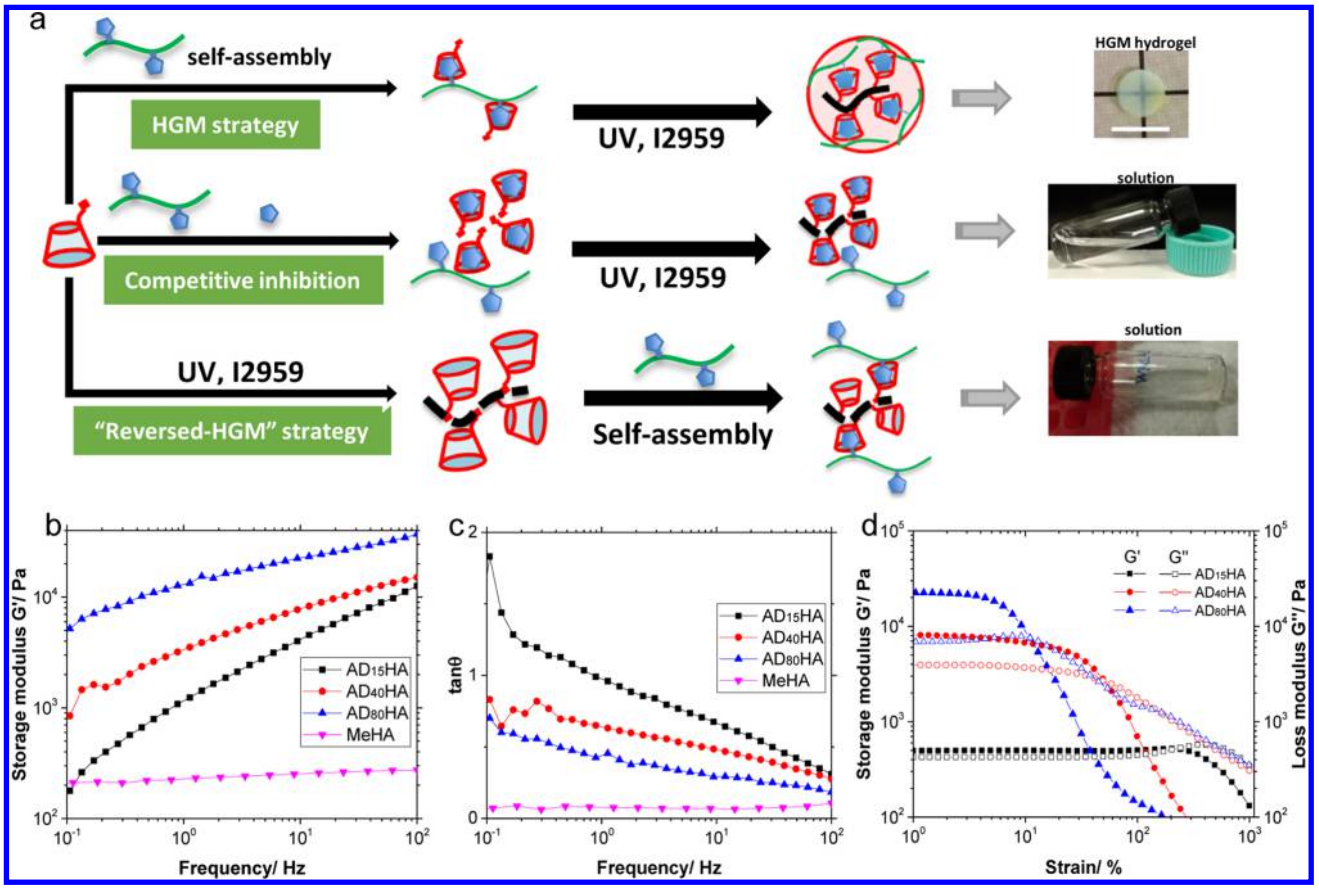

Figure 3. (a) Schematic illustration of the HGM strategy (upper row), inhibition of HGM formation by the competitive guest molecules (middle row), and the reversed-HGM strategy (lower row). Frequency dependency of (b) the storage modulus (G') and (c) the damping factor (tan θ) of the HGM and MeHA hydrogels. (d) The strain sweep of the HGM hydrogels.

irreversible destruction of the static network structure in the chemical hydrogels under compression, the compressive force rearranges the physically associated polymer chains in the dynamic network structure of HGM hydrogels, thereby giving rise to the energy dissipation before breakage of the polymeric networks (Figure 4b). Such energy dissipation is revealed by the stress relaxation analysis (Figure 4c–g).[40] For comparison with chemical MeHA hydrogels (modification degree is 37%), $AD_{40}HA$ is used for HGM hydrogel preparation hereafter. We stepwisely increase the compressive strain and study the stress relaxation behavior in the following 5 min. Compared to the MeHA hydrogels, which slowly relax about 10% of the peak stress in the first 2 min, the HGM hydrogels rapidly relax over 80% of the peak stress during the same time interval at all strain levels (Figure 4c,d). Since the stress relaxation of chemical hydrogels is dominated by migration of water molecules in the static networks, the relaxation curves of MeHA hydrogels are well fitted to an exponential equation (eq 2) where σ_t is the stress at a certain time t, σ_0 is the peak stress, A is a constant, and k_1 is the relaxation rate (Figure 4e).

$$\sigma_t = \sigma_0 + Ae^{-k_1 t} \quad (2)$$

In contrast, the HGM hydrogels can relax the compressive stress by two modes, i.e., the slow mode and the fast mode. Their relaxation curves are well fitted to a double-exponential equation (eq 3)

$$\sigma_t = \sigma_0 + Be^{-k_2 t} + Ce^{-k_3 t} \quad (3)$$

where σ_t and σ_0 are as previously defined, B and C are constants, and k_2 and k_3 are the fast and slow relaxation rate, respectively (Figure 4f).[41] As sumarized in Figure 4g, k_2 is about 1 order of magnitude higher than k_3, and they both show clear strain dependency, indicating that the stress relaxation of the HGM hydrogels are faster at the higher strain levels. Meanwhile, k_3 well matches k_1 at low strains, indicating that the slow relaxation mode dominated by the migration of water molecules also exists in HGM hydrogels as in the chemical hydrogels. We propose that the fast relaxation mode (k_2) of the HGM hydrogels is related to the dissociation of the host–guest complexes, and this is similar to the stress relaxation behavior of a gel with reversible ionic cross-links.[40] After fast stress relaxation mediated by the host–guest dissociation and polymer chain rearragement, the host–guest reassociation happens almost instantaneously, preventing the macroscopic rupture of the HGM hydrogels (Figure 4b). Such rapid host–guest reassociation is revealed by the 3ITT (3-interval time test) experiment (Figure 4h). The storage modulus (G') is higher than the loss modulus (G'') of the HGM hydrogel under a low shear strain (10%). The loading of a high shear strain (300%) immediately disrupts the physical network of the HGM hydrogels, as evidenced by a sharp decrease of G' and G'' and the higher G'' compared to G'. The rapid recovery of the "gel state" upon the removal of high strain reveals the almost instantaneous host–guest reassociation and self-healing of the disrupted physical networks, albeit with a minor decrease in the moduli which may be due to the insufficient rematching

DOI: 10.1021/acs.macromol.5b02527
Macromolecules XXXX, XXX, XXX–XXX

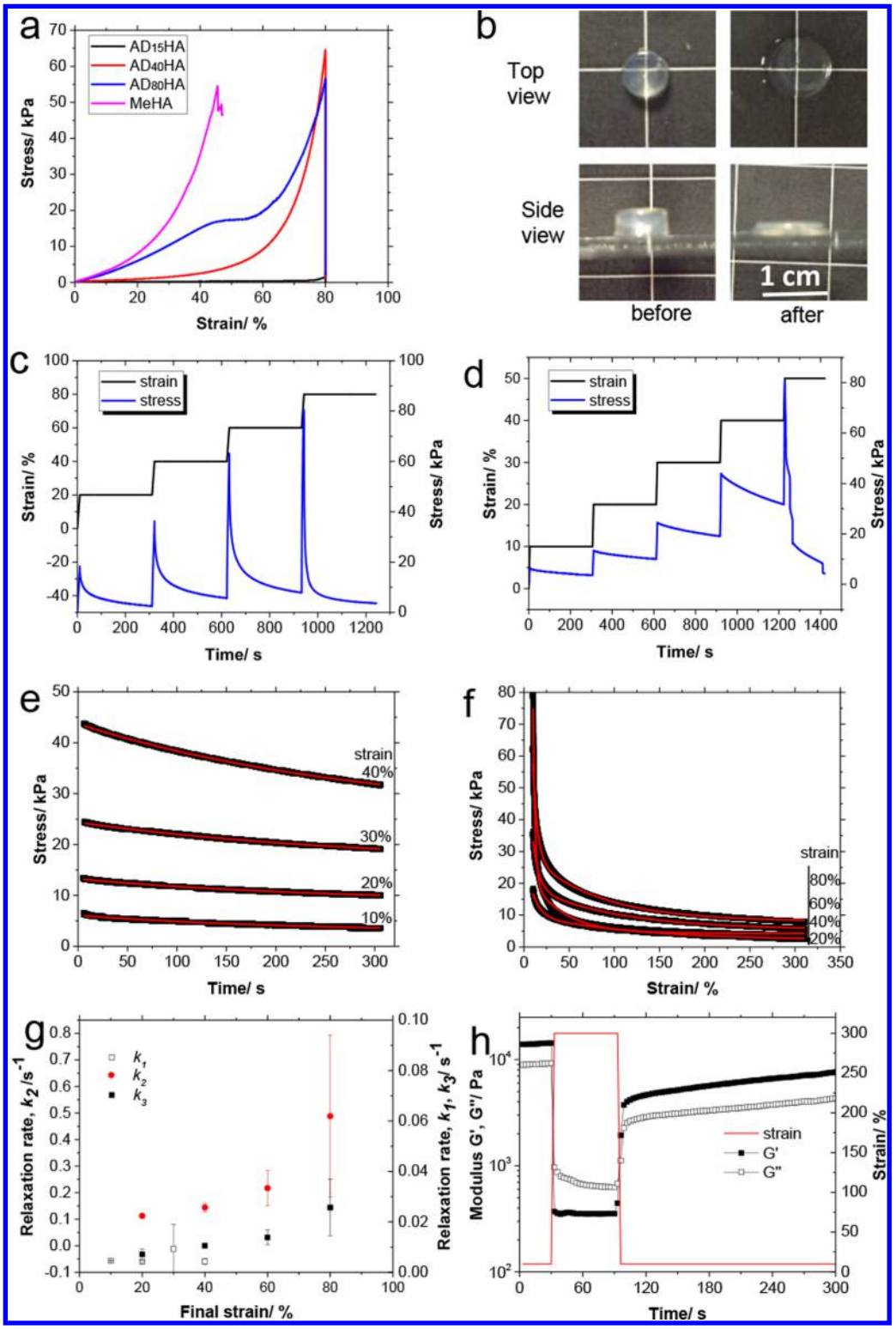

Figure 4. (a) Compressive tests of the HGM and MeHA hydrogels. (b) The top view and the side view of the HGM hydrogels ($AD_{40}HA$) before and after compression. Stress relaxation behavior of (c) the MeHA hydrogel and (d) the HGM hydrogels ($AD_{40}HA$). The exponential fitting of the stress relaxation curves (black: data; red: fitting) of (e) the MeHA hydrogels and (f) the HGM hydrogels ($AD_{40}HA$). (g) The relaxation rates (k_1, k_2, and k_3) depending on the strains. (h) The dynamic rheological 3-interval time test (3ITT) of the HGM hydrogel ($AD_{40}HA$).

between host and guest moieties and the resultant lower effective cross-linking density.

3.3.3. Self-Healing and Easy Moldability of the HGM Hydrogels. Such superior compressibility and fast stress relaxation property facilitate the press-fitting and conforming of the HGM hydrogels into voids of irregular geometries without compromising the hydrogel integrity (Figure 4b). This makes the HGM hydrogels ideal remoldable materials that can better integrate with the surrounding tissues of irregular defects and minimize the mechanical irritation to the surrounding

DOI: 10.1021/acs.macromol.5b02527
Macromolecules XXXX, XXX, XXX−XXX

tissues by relaxing the stress rapidly. To demonstrate this, we use two halves of ruptured HGM hydrogels stained by blue and red dyes, respectively. They can self-heal and reunite to form a new monolithic hydrogel after being kept in contact for 2 min due to the successful restoration of the dissociated host−guest complexes on the interface. Futhermore, the dissociation and restoration of the host−guest interactions allow for the rearrangement of polymer chains in the hydrogel matrix during compression, thereby allowing the self-healed disk-shaped HGM hydrogel to be remolded into a rectangular shape with ease (Figure 5a,b).

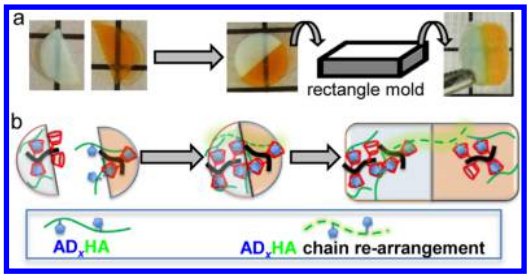

Figure 5. (a) A demonstration of the self-healing and remolding of the HGM hydrogel ($AD_{40}HA$). (b) Schematic illustration of the restoration of host−guest interactions upon the self-healing of two pieces of ruptured HGM hydrogels and the polymer chain rearrangement upon remolding.

3.4. Host−Guest Macromer Hydrogels for Cartilage Regeneration. *3.4.1. Enhanced Chondrogenesis of hMSCs in HGM Hydrogels.* To demonstrate that such HGM hydrogels are promising biomaterials for tissue regeneration, we use HGM hydrogels to encapsulate human mesenchymal stem cells (hMSCs), which are a promising cell source for tissue regeneration due to their potential to differentiate into several mesenchymal lineages including cartilage.[42] The gelation process is found not affected by cells under such conditions, indicating that host−guest complexation is robust enough for cell-related applications. The as-prepared cell-laden hydrogels are then remolded into rectangle shape by press-fitting into a rectangle mold within 2 min (Figure 6a, inset). We evaluate the viability of cells encapsulated in the remolded HGM hydrogels at 24 h after the remolding procedure, and it shows that the majority of cells are viable (Figure S16). Even after 21 days of culture, the majority of the encapsulated hMSCs remain viable (Figure 6a), indicating that the cells are effectively protected by the hydrogel matrix during hydrogel deformation. Moreover, the HGM hydrogels better support the chondrogenesis of the encapsulated hMSCs compared to the MeHA hydrogels likely due to the enhanced retention of growth factors in the HGM hydrogels. Instead of being added continuously to the culture medium, TGF-β1 is encapsulated in the hMSC-laden hydrogels during the hydrogel fabrication. After 7 days of culture in the TGF-β1-free medium, the expression levels of chondrogenic marker genes including type II collagen (COL2), aggrecan (AGG), and sex determining region Y-box 9 (SOX9) are

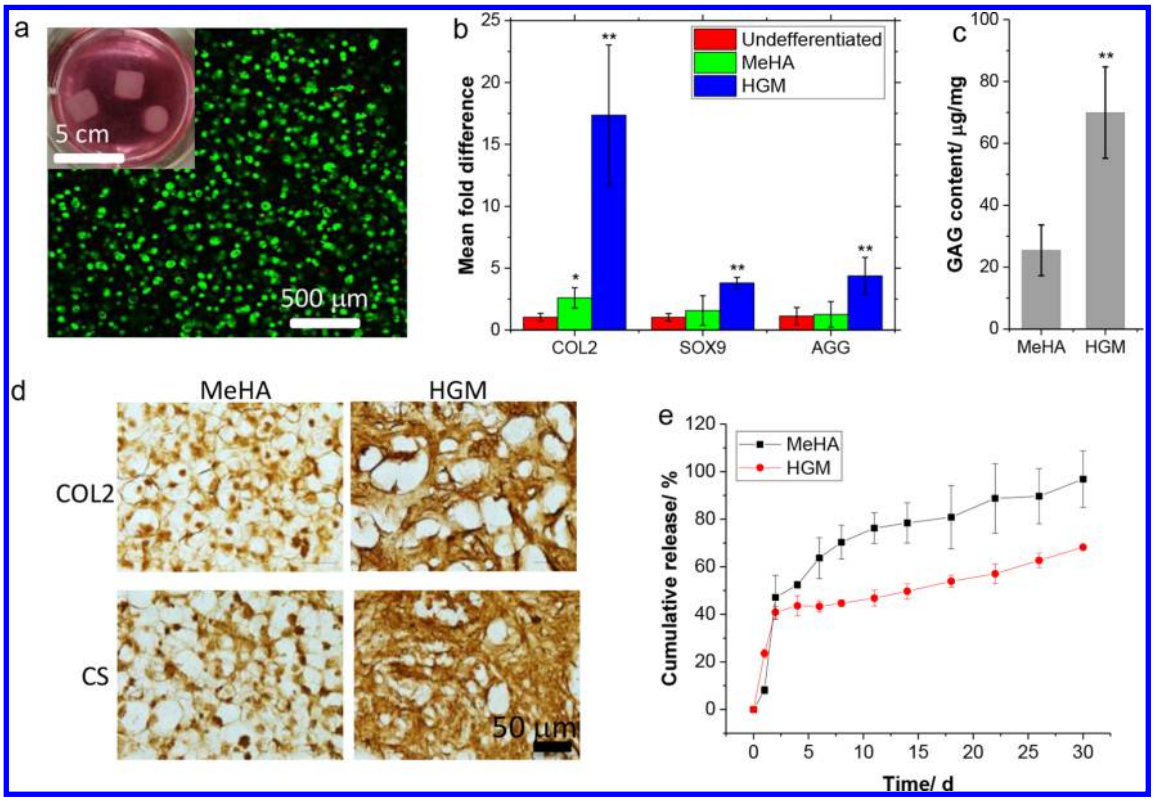

Figure 6. (a) Viability assay of cells encapsulated in the remolded HGM hydrogels after 21 days of culture (green: living cells; red: dead cells; inset: photo of the remolded hMSC-laden HGM hydrogels with rectangle shapes, one original disk like hydrogel is also presented). (b) Gene expression level of type II collagen (COL2), SOX9, and aggrecan (AGG) in hydrogels after 7 days of culture in TGF-β1-free medium. (c) GAG content normalized by total protein content (μg/mg) in hMSC-laden hydrogels after 21 days of culture. (d) Immunohistochemical staining of type II collagen (COL2) and chondroitin sulfate (CS) in hMSC-laden hydrogels after 21 days of culture. (e) Cumulative relase of BSA encapsulated in the MeHA and HGM hydrogels. $^{**}P < 0.005$, $^{*}P < 0.05$ vs the control group ($n = 4$).

DOI: 10.1021/acs.macromol.5b02527
Macromolecules XXXX, XXX, XXX−XXX

significantly elevated in HGM hydrogels (Figure 6b).[27] In contrast, the expression levels of these marker genes in the MeHA hydrogels are not significantly different from those of undifferentiated hMSCs ("undifferentiated") except that the expression of type II collagen (COL2) is slightly increased. Moreover, after 21 days of culture in the TGF-β1-free medium, the glycosaminoglycan (GAG) content in the HGM hydrogels is around 3 times that in the MeHA hydrogels (Figure 6c). Immunohistochemical staining also shows that much more cartilage specific matrix components, including type II collagen (COL2) and chondroitin sulfate (CS), are deposited in the HGM hydrogels than in the MeHA hydrogels (Figure 6d). It is noteworthy that under continuous medium supplementation of TGF-β1 the expression levels of these marker genes in the MeHA hydrogels are also significantly increased (Figure S17), indicating that the fast leakage of TGF-β1 from the MeHA hydrogels is responsible for the poor chondrogenic induction in the TGF-β1-free medium. We postulate that the domains of the host−guest nanoclusters in the HGM hydrogels, which are more hydrophilic than those polyacrylate nanodomains of the MeHA hydrogels, may have contributed to the improved retention of the soluble growth factors within the HGM hydrogels. This speculation is supported by the fact that after a similar initial burst release, which is likely dominated by the release of the proteins trapped outside the nanodomains, the HGM hydrogels release the encapsulated model proteins (bovine serum albumin, BSA) more slowly than the MeHA hydrogels (Figure 6e). Findings from these *in vitro* studies suggest that the HGM hydrogels are more promising than the MeHA chemical hydrogels for *in vivo* applications, where continuous addition of growth factors is impractical.

3.4.2. Cartilage Regeneration in a Rat Model. To confirm the efficacy of our HGM hydrogels *in vivo*, we use the HGM hydrogels to deliver rat mesenchymal stem cells (rMSCs) and chondrogenic growth factors (TGF-β1) for repairing of osteochondral defects in the knees of Sprague−Dawley rats. The hydrogels are prepared with the encapsulation of rMSCs and TGF-β1 as above-mentioned and then implanted in osteochondral defects in the knees of rats. Six weeks after implantation, compared to the control defects treated with the chemical MeHA hydrogels, those treated with our HGM hydrogels show a more congruent and smooth articular surface (Figure 7a, arrows). Histology staining reveals the better regeneration of the subchondral bone in the defects treated with our HGM hydrogels than that treated with the chemical MeHA hydrogels. Moreover, a layer of hyaline cartilage tissue is generated in the defects treated with our HGM hydrogels. This can be ascribed to the unique nanostructures and physical properties of the HGM hydrogels, which enable better retention of TGF-β1 and better integration with the surrounding tissues.

4. CONCLUSION

We have developed the HGM approach for preparing supramolecular hydrogels reinforced by *in situ* formed multivalent host−guest nanoclusters as the cross-linking junctions of biopolymers. Such HGM approach combines the efficient host−guest complexation and *in situ* clustering of the host−guest complexes, thus producing robust HGM hydrogels. Our HGM hydrogels are robust enough as reswellable freestanding 3D constructs and retain useful physical properties. By virtue of the reversible host−guest interactions, our HGM hydrogels are self-healable and compressible. They can relax the compressive stress rapidly via fast host−guest dissociation and afford effective protection on the encapsulated stem cells during the compression remolding, making them promising biomaterial that can quickly adapt to and integrate with surrounding tissues of the targeted defects. Furthermore, the HGM hydrogels reduce the fast leakage of the encapsulated growth factors, leading to the enhanced chondrogenesis of hMSCs and neocartilage formation. A preliminary *in vivo* study shows that our HGM hydrgogels better support cartilage resurfacing in a rat model compared to conventional chemically cross-linked hydrogels. These results demonstrate that the HGM hydrogels are promising carrier materials of stem cells and therapeutic agents for tissue repair and regeneration.

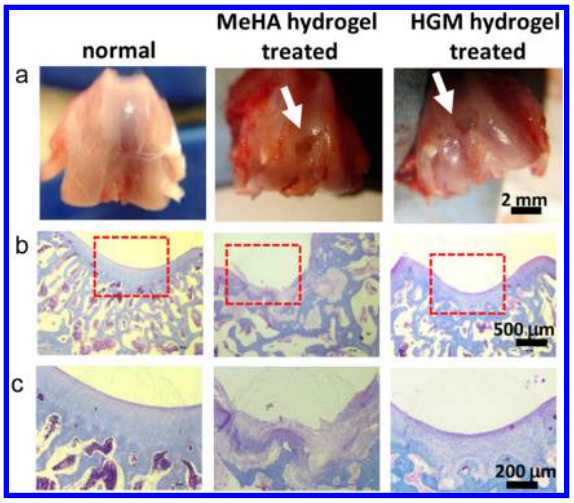

Figure 7. (a) Photos of the knee cartilage surface of rats, from left to right: normal cartilage, cartilage with defect (white arrows) treated by implanting MeHA hydrogel or HGM hydrogel loaded with rMSCs and TGF-β1 for 6 weeks. (b) Safranin O/fast green staining of the histological sections of the cartilage defects after 6 weeks of healing presented in panel a. (c) Partial enlargement of the areas marked with red-dashed lines in panel b (n = 4 for each group).

■ ASSOCIATED CONTENT

Supporting Information

The Supporting Information is available free of charge on the ACS Publications website at DOI: 10.1021/acs.macromol.5b02527.

Additional synthesis methods, NMR characterization, swelling behaviors of the HGM hydrogels, chondrogenic differentiation of hMSCs in MeHA hydrogels (PDF)

■ AUTHOR INFORMATION

Corresponding Author

*E-mail: lbian@mae.cuhk.edu.hk (L.B.).

Funding

The work described in this paper is supported by a General Research Fund grant from the Research Grants Council of Hong Kong (Project No. 14202215). This research is also supported by project BME-p3-15 of the Shun Hing Institute of Advanced Engineering, The Chinese University of Hong Kong; the Health and Medical Research Fund, the Food and Health Bureau, the Government of the Hong Kong Special Administrative Region (reference no.: 02133356). Project 31570979 is supported by the National Natural Science Foundation of China.

DOI: 10.1021/acs.macromol.5b02527
Macromolecules XXXX, XXX, XXX−XXX

Notes

The authors declare no competing financial interest.

■ ACKNOWLEDGMENTS

We thank Dr. Lei Xu for his assistance in rheological studies, Dr. Zigang Li for his help in ITC studies, and Ms. Ye Hong and Mr. Yifei Yao for the compression tests.

■ REFERENCES

(1) Balakrishnan, B.; Banerjee, R. *Chem. Rev.* **2011**, *111*, 4453−4474.
(2) Van Vlierberghe, S.; Dubruel, P.; Schacht, E. *Biomacromolecules* **2011**, *12*, 1387−1408.
(3) Stella, J. A.; D'Amore, A.; Wagner, W. R.; Sacks, M. S. *Acta Biomater.* **2010**, *6*, 2365−2381.
(4) Seiffert, S.; Sprakel, J. *Chem. Soc. Rev.* **2012**, *41*, 909−930.
(5) Appel, E. A.; Barrio, J.; Loh, X. J.; Scherman, O. A. *Chem. Soc. Rev.* **2012**, *41*, 6195−6214.
(6) Frantz, C.; Weaver, V. M.; Weaver, V. M. *J. Cell Sci.* **2010**, *123*, 4195−4200.
(7) Park, K. M.; Yang, J. A.; Jung, H.; Yeom, J.; Park, J. S.; Park, K. H.; Hoffman, A. S.; Hahn, S. K.; Kim, K. *ACS Nano* **2012**, *6*, 2960−2968.
(8) Jung, H.; Park, J. S.; Yeom, J.; Selvapalam, N.; Park, K. M.; Oh, K.; Yang, J. A.; Park, K. H.; Hahn, S. K.; Kim, K. *Biomacromolecules* **2014**, *15*, 707−714.
(9) Brochu, A. B. W.; Craig, S. L.; Reichert, W. M. *J. Biomed. Mater. Res., Part A* **2011**, *96A*, 492−506.
(10) Guvendiren, M.; Lu, H. D.; Burdick, J. A. *Soft Matter* **2012**, *8*, 260−272.
(11) Rodell, C. B.; Kaminski, A. L.; Burdick, J. A. *Biomacromolecules* **2013**, *14*, 4125−4134.
(12) Ye, E. Y.; Chee, P. L.; Prasad, A.; Fang, X. T.; Owh, C.; Yeo, V. J. J.; Loh, X. J. *Mater. Today* **2014**, *17*, 194−202.
(13) Burdick, J. A.; Murphy, W. L. *Nat. Commun.* **2012**, *3*, 1269.
(14) Appel, E. A.; Tibbitt, M. W.; Webber, M. J.; Mattix, B. A.; Veiseh, O.; Langer, R. *Nat. Commun.* **2015**, *6*, 6295.
(15) Sun, Z. F.; Lv, F. C.; Cao, L. J.; Liu, L.; Zhang, Y.; Lu, Z. G. *Angew. Chem., Int. Ed.* **2015**, *54*, 7944−7948.
(16) Charlot, A.; Heyraud, A.; Guenot, P.; Rinaudo, M.; Auzely-Velty, R. *Biomacromolecules* **2006**, *7*, 907−913.
(17) Charlot, A.; Auzely-Velty, R. *Macromolecules* **2007**, *40*, 9555−9563.
(18) Charlot, A.; Auzely-Velty, R. *Macromolecules* **2007**, *40*, 1147−1158.
(19) Tan, S.; Ladewig, K.; Fu, Q.; Blencowe, A.; Qiao, G. G. *Macromol. Rapid Commun.* **2014**, *35*, 1166−1184.
(20) Hashidzume, A.; Harada, A. *Polym. Chem.* **2011**, *2*, 2146−2154.
(21) Kakuta, T.; Takashima, Y.; Harada, A. *Macromolecules* **2013**, *46*, 4575−4579.
(22) Kakuta, T.; Takashima, Y.; Nakahata, M.; Otsubo, M.; Yamaguchi, H.; Harada, A. *Adv. Mater.* **2013**, *25*, 2849−2853.
(23) Khetan, S.; Guvendiren, M.; Legant, W. R.; Cohen, D. M.; Chen, C. S.; Burdick, J. A. *Nat. Mater.* **2013**, *12*, 458−465.
(24) Khetan, S.; Burdick, J. A. *Biomaterials* **2010**, *31*, 8228−8234.
(25) Hanjaya-Putra, D.; Wong, K. T.; Hirotsu, K.; Khetan, S.; Burdick, J. A.; Gerecht, S. *Biomaterials* **2012**, *33*, 6123−6131.
(26) Nichol, J. W.; Koshy, S. T.; Bae, H.; Hwang, C. M.; Yamanlar, S.; Khademhosseini, A. *Biomaterials* **2010**, *31*, 5536−5544.
(27) Nguyen, K. T.; West, J. L. *Biomaterials* **2002**, *23*, 4307−4314.
(28) Bian, L. M.; Guvendiren, M.; Mauck, R. L.; Burdick, J. A. *Proc. Natl. Acad. Sci. U. S. A.* **2013**, *110*, 10117−10122.
(29) Kloxin, A. M.; Kloxin, C. J.; Bowman, C. N.; Anseth, K. S. *Adv. Mater.* **2010**, *22*, 3484−3494.
(30) Anseth, K. S.; Bowman, C. N.; Brannon, P. L. *Biomaterials* **1996**, *17*, 1647−1657.
(31) Fairbanks, B. D.; Schwartz, M. P.; Halevi, A. E.; Nuttelman, C. R.; Bowman, C. N.; Anseth, K. S. *Adv. Mater.* **2009**, *21*, 5005−5010.
(32) Alberts, B.; Johnson, A.; Lewis, J.; Raff, M.; Roberts, K.; Walter, P. *Molecular Biology of the Cell*, 4th ed.; Garland Science: New York, 2002.
(33) Rekharsky, M. V.; Inoue, Y. *Chem. Rev.* **1998**, *98*, 1875−1917.
(34) Chen, G.; Jiang, M. *Chem. Soc. Rev.* **2011**, *40*, 2254−2266.
(35) Guo, M. Y.; Jiang, M.; Zhang, G. Z. *Langmuir* **2008**, *24*, 10583−10586.
(36) Wei, K. C.; Li, J.; Chen, G. S.; Jiang, M. *ACS Macro Lett.* **2013**, *2*, 278−283.
(37) Waters, D. J.; Engberg, K.; Parke-Houben, R.; Hartmann, L.; Ta, C. N.; Toney, M. F.; Frank, C. W. *Macromolecules* **2010**, *43*, 6861−6870.
(38) Xia, L. W.; Xie, R.; Ju, X. J.; Wang, W.; Chen, Q. M.; Chu, L. Y. *Nat. Commun.* **2013**, *4*, 2226.
(39) Cleland, R. L. *Arch. Biochem. Biophys.* **1977**, *180*, 57−68.
(40) Zhao, X. H.; Huebsch, N.; Mooney, D. J.; Suo, Z. G. *J. Appl. Phys.* **2010**, *107*, 107.
(41) Lv, S.; Dudek, D. M.; Cao, Y.; Balamurali, M. M.; Gosline, J.; Li, H. B. *Nature* **2010**, *465*, 69−73.
(42) Caplan, A. I. *J. Orthop. Res.* **1991**, *9*, 641−650.
(43) Li, G.; Tajima, H.; Ohtani, T. *J. Org. Chem.* **1997**, *62*, 4539−4540.
(44) Pochan, D. J.; Pakstis, L.; Ozbas, B.; Nowak, A. P.; Deming, T. J. *Macromolecules* **2002**, *35*, 5358−5360.

DOI: 10.1021/acs.macromol.5b02527
Macromolecules XXXX, XXX, XXX−XXX